J.Grzyb, K. Gieczewska, J. Łabuz, O.Sztatelman, BBA-Biomembranes, 1860:281-291, 2018
Accepted manuscript
https://doi.org/10.1016/j.bbamem.2017.10.012

Title: Detailed characterization of *Synechocystis* PCC 6803 ferredoxin:NADP$^+$ oxidoreductase interaction with model membranes

Joanna Grzyb[1,2*], Katarzyna Gieczewska[3,4], Justyna Łabuz[5], Olga Sztatelman[6]

[1]Department of Biophysics, Faculty of Biotechnology, University of Wroclaw, F. Joliot Curie 14a, 50-383 Wroclaw, Poland

[2]Laboratory of Biological Physics, Institute of Physics Polish Academy of Sciences, Aleja Lotników 32/46, PL-02668 Warsaw, Poland

[3]Department of Plant Anatomy and Cytology, Faculty of Biology, University of Warsaw, Miecznikowa 1, PL-02096 Warsaw, Poland

[4]Department of Biophysics, Institute of Physics, Maria Sklodowska-Curie University, M. Sklodowska-Curie sq. 5, PL-20031 Lublin, Poland

[5]Malopolska Centre of Biotechnology, Jagiellonian University, Gronostajowa 7A, PL-30387 Krakow, Poland.

[6]Department of Plant Biochemistry, Institute of Biochemistry and Biophysics, Polish Academy of Sciences, Pawińskiego 5a, PL-02106 Warszawa, Poland

*joanna.grzyb@uwr.edu.pl

Abstract:

Direct interaction of ferredoxin:NADP+ oxidoreductase (FNR) with thylakoid membranes was postulated as a part of the cyclic electron flow mechanism. In vitro binding of FNR to digalactosyldiacylglycerol and monogalactosyldiacylglycerol membranes was also shown. In this paper we deal with the latter interaction in more detail describing the effect for two FNR forms of Synechocystis PCC 6803. The so-called short FNR (sFNR) is homologous to FNR from higher plant chloroplasts. The long FNR (lFNR) form contains an additional domain, responsible for the interaction with phycobilisomes. We compare the binding of both sFNR and lFNR forms to native and non-native lipids. We also include factors which could modulate this process: pH change, temperature change, presence of ferredoxin, NADP+ and NADPH and heavy metals. For the lFNR, we also include phycobilisomes as a modulating factor. The membrane binding is generally faster at lower pH. The sFNR was binding faster than lFNR. Ferredoxin isoforms with higher midpoint potential, as well as NADPH and NADP+, weakened the binding. Charged lipids and high phosphate promoted the binding. Heavy metal ions decreased the rate of membrane binding only when FNR was preincubated with them before injection beneath the monolayer. FNR binding was limited to surface lipid groups and did not influence hydrophobic chain packing. Taken together, FNR interaction with lipids appears to be non-specific, with an electrostatic component. This suggests that the direct FNR

interaction with lipids is most likely not a factor in directing electron transfer, but should be taken into account during *in vitro* studies.

Introduction

Ferredoxin-$NADP^+$ oxidoreductase (FNR) is a photosynthetic enzyme that transfers electrons from reduced ferredoxin to $NADP^+$, forming NADPH [1] (Supplementary, Fig. S-1). This definition describes classic (chloroplastic-like) FNR involved in linear electron transfer in plant leaves or cyanobacteria cells. Leaf FNR is a monomer of ca. 36 kDa consisting of two domains (Fig. S-1a). One of them contains the NAD(P) binding motif. The cofactor of FNR, flavine adenine dinucleotide (FAD), is bound non-covalently in the narrow space between the two domains. In Cyanobacteria, two isoforms of FNR (lFNR and sFNR) are found. Cyanobacterial FNR has an additional, N-terminal domain homologous to phycocyanin associated linker protein (CpcD). This domain is responsible for binding to phycobilisomes [2]. Phycobilisomes (PBS) are huge pigment-protein complexes, which play a role of photosynthetic antennae in Cyanobacteria. Oppositely to light harvesting complexes of higher plants, which are internal membrane complexes, PBS are water soluble and attach to photosystems on the membrane surface. In some conditions, FNR may exist in both forms (e.g. under salt stress [2].

FNR is encoded by a nuclear gene, *petH,* and in higher plants a premature version of a protein contains an N-terminal peptide that targets the protein to chloroplasts [3]. Over the years, several papers have reported co-purification of FNR with various thylakoid complexes and the involvement of this enzyme in cyclic electron transfer. These claims have later been proven wrong [2, 4-10]. Finally, Iwai et al. [11] has shown the functional and structural involvement of FNR in cyclic electron transfer supercomplex. TROL (thylakoid rhodanase-like protein) has been postulated to specifically participate in FNR binding to the thylakoid membrane in *Arabidopsis thaliana* [12, 13]. Tic62, an *A. thaliana* integral membrane protein, also binds FNR [14, 15]. In general, FNR may interact with several partners. Such interactions are regulated in accordance to the redox state of chloroplast stroma [14]. The main partner of photosynthetic FNR is ferredoxin (Fd). Fd is a small, water soluble protein, carrying an [2Fe2S] iron-sulfur cluster. Fd takes an electron from photosystem I and transfers it to FNR. The main photosynthetic Fd has a midpoint potential (E_m) of about – 400 mV, however there are also isoforms with higher E_m, playing different roles, e.g. in sulfite reduction, non-linear electron transfer or signaling [16]. In non-photosynthetic plastids so-called non-photosynthetic FNR isoforms have been identified. For example in root tissues, FNR plays a role in nitrogen fixation and other biosynthetic processes that require reduced ferredoxin. In that case, FNR uses NADPH as a source of electrons for the reduction process. There are also isoforms of FNR, which are localized outside plastids. A cytosolic isoform of FNR, which plays a role of nitric oxide dioxygenase for hemoglobin, was found recently in poplar [17]. There are also reports that photosynthetic spinach FNR may reduce a quinone substrate [18-20]. This suggests the importance of the reaction *in vivo*. FNR isolated with cytochrome b_6f complex is also able to reduce quinones [21]. Since quinones are hydrophobic, they were exposed to the enzyme in detergents or incorporated into liposomes. We have shown [22] that FNR binds directly to lipids (monogalactosyldiacylglicerol, MGDG and digalactosyldiacylglicerol, DGDG) in a pH dependent manner. This binding results in a partial incorporation of FNR into the lipid bilayer and at the same time increases the NADPH oxidation rate with an artificial quinone as a substrate. These facts may suggest that FNR binds to lipids and reduces the

quinone substrate present there and that its interaction with other proteins is only auxiliary. Again, a question rises – is the interaction with lipids really physiological or is it just a side effect of FNR surface's adaptation to interacting with several partners.

A temporary, reversible attachment to the membrane is a common mechanism regulating the activity of enzymes, which recognize hydrophobic and available in membrane substrates. This process may be regulated by phosphorylation. The Ras-like GTP binding protein rab4, a protein involved in regulation of the cell cycle, is soluble when phosphorylated, but after dephosphorylation it associates with the cell membrane [24]. Acylation may also induce membrane binding as in the case of the ras protein in mammalian fibroblasts. A change in pH, inducing protonation/deprotonation and in parallel, a change in the protein charge, induces membrane binding in hisactophilin, a cytoskeletal linker protein in slime molds. Ligand binding regulates the membrane attachment of proteins containing Pleckstrin Homology (PH) domains which bind diacylglycerol [25].

Photosynthetic membranes are composed of lipids and pigment-protein complexes. In this paper, we focused on FNR interaction with the first ones. MGDG, DGDG, sulfoquinovosyldiacylglycerol (SQDG) and phosphatidylglycerol (PG) are membrane lipids native to FNR. The first two constitute at least 75% of all photosynthetic membrane lipids [26]. MGDG and DGDG are galactolipids, with mono- and digalactose moieties as polar head groups, respectively. These groups significantly change the packing parameter and the tendency to form bilayers. DGDG is a bilayer forming lipid, while MGDG creates reverse micelles. This difference is important for thylakoid membrane organization, as MGDG helps huge protein complexes such as photosystems and light harvesting complexes to incorporate into the bilayer structure [27]. MGDG, by disturbing the packing of the bilayer and, in consequence, by forming inverted hexagonal structures (H_{II}) is also important for violaxanthin deepoxidation. It enables to expose the second ring of the violaxanthin molecule to the violaxanthin deepoxidase enzyme [28] and it is essential for the activity of light-dependent protochlorophyllide oxidoreductase [29]. In natural membranes, including thylakoids, charged lipids have also been identified. One of them is phosphatidylglycerol (PG), containing a not neutralised negative charge on its phosphate group. The second one is SQDG, also with a negative charge on a sulphur group. SQDG is a structural lipid of pigment-protein complexes. PG and SQDG form bilayers. In numerous research approaches, phosphatidylcholine (PC) is used as a control for bilayer forming lipids, see e.g. [30, 31]. In model membrane studies the most commonly used version of PC is dipalmitoylphosphatidylcholine (DPPC) due to its ubiquity in animal membranes. The bilayer created by DPPC is 4.8 ± 0.3 nm thick [32], which is slightly thicker than the plasma membrane [33]. The second most used PC derivative is dimyristoylphosphatidylcholine (DMPC). DMPC differs from DPPC by the length of its acyl group (14 C versus 16 C), which results in a thinner bilayer. All PC derivatives, as well as galactolipids, are neutral. Phosphatidylcholine has partial charges (negative and positive) on its molecule, which results in a different molecular dipole than that in galactolipids. Their acyl chains are highly unsaturated, and consist mostly of linolenic acid (18:3) [34].

The aim of our study was to examine the binding of FNR to membranes in a model system, taking into account the most possible factors which may regulate these interactions. The second goal was to identify lipid specific interaction places. We used the enzyme from *Synechocystis PCC 6803* as a model FNR, in its short and long form [35]. Both forms were expressed in *Escherichia coli* and purified by affinity chromatography to nickel beads, followed by ion exchange, to reduce to minimum the chance of contamination by lipids, especially the plant ones. In binding tests we used lipids native to FNR, MGDG,

DGDG, SQDG and PG, as well as other non-thylakoid lipids, DMPC, DPPC and DOTAP as controls for comparison of head group properties: their type, volume and molecular charge (Supplementary, Fig. S-2). DPPC was investigated as a model of a bilayer forming lipid. We used DMPC to check whether the length of acyl chains is important for the FNR - membrane interaction. We also included a positively charged lipid, 1,2-dioleoyl-3-trimethylammonium-propane (DOTAP). This lipid is non-natural, but it is widely used in science, eg. in transfection protocols, due to its strong affinity to negatively charged DNA. DOTAP packing parameter suggests preferable bilayer formation. Here we used it to check if FNR binds to non-native, positively charged lipids. We also included other factors, which may act as switches between linear and cyclic electron transfer, and therefore possibly influence FNR binding. The first factor examined was the presence of ferredoxin. We used *Arabidopsis thaliana* Fd2 (a typical photosynthetic isoform) and Fd4 (the one with higher E_m, involved in other processes), as models. As phycobilisomes contain an lFNR binding place and may prevent binding of the enzyme to the membrane, we used phycobiliosmes in one of the experiments. The change of pH, as well as the addition of NADPH or $NADP^+$ simulated two extreme physiological states, after prolonged darkness (pH 8 and $NADP^+$) or under strong illumination (pH 5 and NADPH). We also tested temperature as a possible regulating factor. Finally, we analysed the influence of selected heavy metals (cadmium, copper and zinc), as they may alter electron transfer in thylakoid membranes.

Materials and methods

Proteins

Experiments were carried on two FNR forms from *Synechocystis* PCC6803: the short (sFNR) and long form (lFNR) containing an additional CpcD domain. sFNR and lFNR genes were amplified from *Synechocystis PCC 6803* genomic DNA, cloned into pET28 and expressed in *E.coli*.

Ferredoxin expressed in *E. coli*. For heterologous expression, Fd genes (Fd2, redox potential close to spinach Fd, and Fd4, redox potential about - 150 mV [16]) were amplified from cDNA of *A. thaliana* and cloned into the pET32b vector, with a thioredoxin tag. List of primers used for FNRs and Fds cloning may be found in Supplementary Table S-I. Ferredoxins were used without tag removal.

Phycobilisomes were isolated from *Synechocystiss PCC 6803* cells, by breaking up in liquid nitrogen and resuspension in 0.75 M phosphate buffer, pH 7.5. Whole phycobilisome complexes were purified on a sucrose gradient [36].

Lipids

MGDG, DGDG, PG and SQDG were purchased from Lipid Products, UK. PC, DPPC, DOPG, DOPC, DMPC and DOTAP came from Avanti Polar Lipids, USA.

Langmuir-Blodgett (L-B) experiments

Monolayers of lipids were formed in a Teflon trough, equipped with a magnetic stirrer, filled with 12.5 ml of buffer (25 mM MES/NaOH pH 5.0 or 25 mM HEPES/NaOH pH 8.0). Lipids were deposited from a chloroform stock (~ 1 mg/ml) in several steps, until desired π was reached. Surface pressure was monitored by a tensiometer (Nima Technologies Ltd.). Proteins and other factors were injected beneath the preformed, stabilized monolayer with a microsyringe. Most of LB experiments were done at room temperature. For studies of temperature influence on the binding rate, the whole apparatus was placed in a thermostated chamber and adapted to a given temperature.

To calculate the rate of π increase, a tangent to the curve at the time of the FNR addition was found. For Δπ, the amplitude between the baseline before protein addition and the plateau phase reached after the saturation of protein binding, was determined. For curves without a clear plateau, the maximum was fitted by an asymptotic exponential function, $y = a-b*c^x$, where a is the maximum value, b and c are curve parameters, which are not used in further analysis

To measure pressure-area isotherms, 240 cm^2 of the Teflon trough was used. The trough was filled with an appropriate buffer (225 ml of 25 mM MES/NaOH pH 5.0 or 25 mM HEPES/NaOH pH 8.0) and the lipids were deposited from a chloroform stock, in small drops all over the surface. The formed monolayer was compressed with a mowing barrier (25 mm/min). To investigate the protein influence on isotherms, the monolayer was compressed to 10 mN/m and the barrier was stopped. sFNR (200 µl of 5 µM stock) was then injected below the monolayer in a few aliquots in different positions of the trough. The system

remained stopped to allow for sFNR-membrane binding for about 30 min (till the plateau was reached) and then the compression continued until a collapse was obtained.

Gel filtration

Analysis of complexes and the protein size was performed on a gel filtration column, Superdex G-200 5/150 (GE Healthcare), connected to Akta Purifier (GE Healthcare). Samples were loaded by a 100 µl loop. Separation was monitored spectrophotometrically, by a simultaneous measurement at three independent wavelengths (280 nm, 350 nm and 459 nm). Separation was done with a flow rate of 0.5 ml.

Electrophoresis

Electrophoretic analysis was performed on 12% SDS-PAGE in the Laemmli system. For native conditions, SDS was omitted during gel and buffer preparations. Samples for native page were mixed with the loading dye (1% glycerol and 0.05% bromophenol blue) and directly loaded into gel wells.

Liposomes

Multilamellar vesicles (MLV) were prepared from appropriate lipid mixtures dried on tube walls and hydrated with a chosen buffer (25 mM MES/NaOH pH 5.0 or 25 mM HEPES/NaOH pH 8.0). Small unilamellar vesicles (SUV) were obtained from MLV by sonication. The hydration and sonication were done at room temperature, except for DPPC, for which the temperature was elevated above the transition temperature. For fluorescence anisotropy measurements, diphenylhexatriene (DPH) (Sigma-Aldrich Co.) was added to the lipid mixture before drying (the DPH:lipid mass ratio was 1:200).

FNR activity measurements

FNR activity was determined in the Fd-dependent cytochrome c reduction assay. Cyt c reduction was followed spectrophotometrically (Cary Bio50, Varian) working in a kinetic mode, at 550 nm. The reaction was carried on in a thermostated (22^{o}C) 1 ml quartz cuvette. The baseline was recorded using a mixture containing 10 µM cytochrome c and 20 µM NADPH in a 25 mM HEPES/NaOH buffer pH 8.0, with or without 0.35 µM ferredoxin. The reaction started by FNR addition to the final concentration of 0.025 µM. To test the influence of lipids, 5 µl of 5 µM FNR was mixed with 50 µM of MLV (200 µM lipid concentration, prepared in the reaction buffer), incubated at room temperature for 5 min, and then used to start the reaction. In the control reaction, FNR was mixed with the buffer without the liposomes. The electron transfer rate was calculated as the initial rate of cytochrome c reduction (the tangent to the curve at t=0).

Fluorescence studies

Tryptophan fluorescence of sFNR and lFNR were analyzed by steady state measurements with Cary Eclipse (Agilent, Gmbh) spectrofluorometer. The protein solution (25 nM) in the appropriate buffer (25 mM MES/NaOH pH 5.0 or 25 mM HEPES/NaOH pH 8.0) was placed in a 4 ml quartz cuvette with stirring and thermostated at 22^{o}C. The excitation wavelength was set at 280 nm. Emission was recorded in the range of 300 – 600 nm, with a 1 nm resolution. Emission and excitation slits were 5 nm. In a typical

experiment with heavy metals, the metal salt solution was added to the cuvette just after the first spectrum was recorded, then the measurements were taken every 1 min for the following 30 min (in an automatic mode).

The DPH anisotropy was measured with the Cary Eclipse (Agilent, Gmbh) spectrofluorometer, equipped with a set of polarizers. The cuvette contained SUV in the appropriate buffer (25 mM MES/NaOH pH 5.0 or 25 mM HEPES/NaOH pH 8.0) and FNR. The extinction wavelength was set at 350 nm. Emission spectra were recorded in the range of 370 – 550 nm. The fluorescence intensity at the maximum (425 nm) was used to calculate the anisotropy (*r*) using the following equation:

$$r = \frac{I_{\parallel} - I_{\perp}}{I_{\parallel} + 2I_{\perp}}$$

Where $I_{\parallel}$ is the fluorescence intensity measured in the plane parallel to the excitation and $I_{\perp}$ is the fluorescence intensity measured in the plane perpendicular to the excitation.

Fourier transform infrared spectroscopy (FTIR).

FTIR measurements were performed on proteins deposited as a hydrated film on the surface of a ZnSe crystal. Spectra were recorded with a Bruker Vector 33 spectrometer in an attenuated total reflection (ATR) mode, in dry air atmosphere, with a 0,4 cm^{-1} spectral resolution. For each background and each spectrum 50 interferograms were averaged and Fourier transformed. Data analysis was carried out with Grams/AI 8.0 Spectroscopy Software (Thermo Electron Corporation, USA).

Protein modeling

Protein modeling was done using the Swiss Model automated platform [37, 38]. *Synechococcus* FNR (pdb: 2b5o) was used as a model for sFNR due to its closest sequence homology. *Mastigocladus laminosus* allophycocyanin (pdb: 1b33, [39]) was used as a model for the cpcD-like domain of IFNR. Surface electrostatic potential was simulated with Swiss PdbViewer [40] assuming the default protonation of the protein at pH 7, the dielectric constant of solvent 80, the dielectric constant of protein 4 and the solvent ionic strength 50 mM.

Results

The interaction of FNR with lipids was examined by injection of the protein under Langmuir-Blodgett monolayer formed from a given lipid. The concentration of FNR, used in the following experiments (15 nM), was selected in preliminary tests with injections beneath L-B monolayers formed from MGDG. Lower concentrations of FNR did not cause any effect as compared with the control (the buffer injection). MGDG was used to determine the FNR concentration because in the previous paper [22] the greatest π changes were observed after injection of the spinach FNR beneath the monolayer built of this lipid.

Analysis of FNR-lipid interaction with the LB method

Injection of sFNR beneath the monolayer formed from MGDG, DGDG, DPPC, DOTAP, DOPG, SQDG, as well as mixtures of MGDG/DGDG or MGDG/DPPC resulted in a gradual increase of π, until a plateau phase was reached (see Supplementary, Fig. S-3). The results obtained for MGDG and DGDG correspond with observations made for spinach FNR [22]. Fig. 1 compares the rate of initial π changes and the maximum change of π for sFNR injected beneath selected lipid monolayers for two pH values and for two different starting π values.

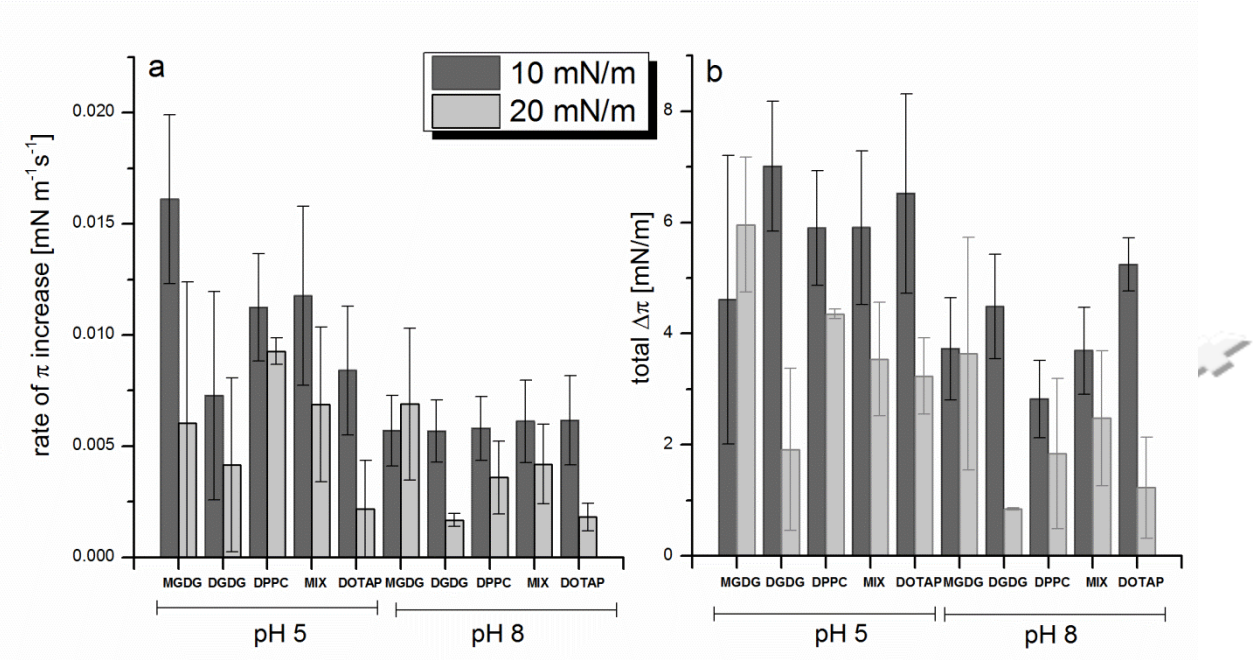

Fig. 1. The sFNR injection beneath the lipid monolayer: a comparison of the rate of initial π increase (a) and the total change in π (b) for selected composition of the monolayer (MGDG, DGDG, DPPC or mixed – 30% MGDG/70% DGDG) and two starting π values (10 mN/m or 20 mN/m) and at pH 5 or pH 8. Error bars – SD from 3-4 independent repetitions.

The highest initial rate of the π increase was found for the injection beneath the MGDG monolayer at pH 5, for the lower starting π value (10 mN/m). Total Δπ was the highest for DGDG at pH 5, despite the low initial rate. For higher initial packing of the membrane (20 mN/m), the binding of the protein was hindered, both for the sugar and phosphatidylcholine type of the lipid hydrophilic head. sFNR was also

bound to other tested lipids (see Supplementary, Fig. S-3). A general rule was a faster binding rate at pH 5 than at pH 8. It was not changed in the presence of charged lipid head groups.

lFNR was also bound to membranes, however with a lower binding rate than sFNR (Fig. 2, Fig. S-3). The binding to all tested lipids was faster at pH 5 than at pH 8. There was a difference in the relative ratio between lipids. Binding to MGDG was the fastest, however binding to DOTAP reached the same rate value. DGDG binding rate was the third. The slowest binding was found when DPPC was used. This suggests that the CpcD domain even counteracted the interaction with lipids. Most probably ionic interactions (between lipid head groups and charged protein patches) were weakened because of higher pI of lFNR (pI 5.72) in comparison with sFNR (pI 5.27). There is also a possibility, due to the change in the binding rate observed also for neutral lipids, that the CpcD domain screened those parts of the FNR surface which are involved in binding.

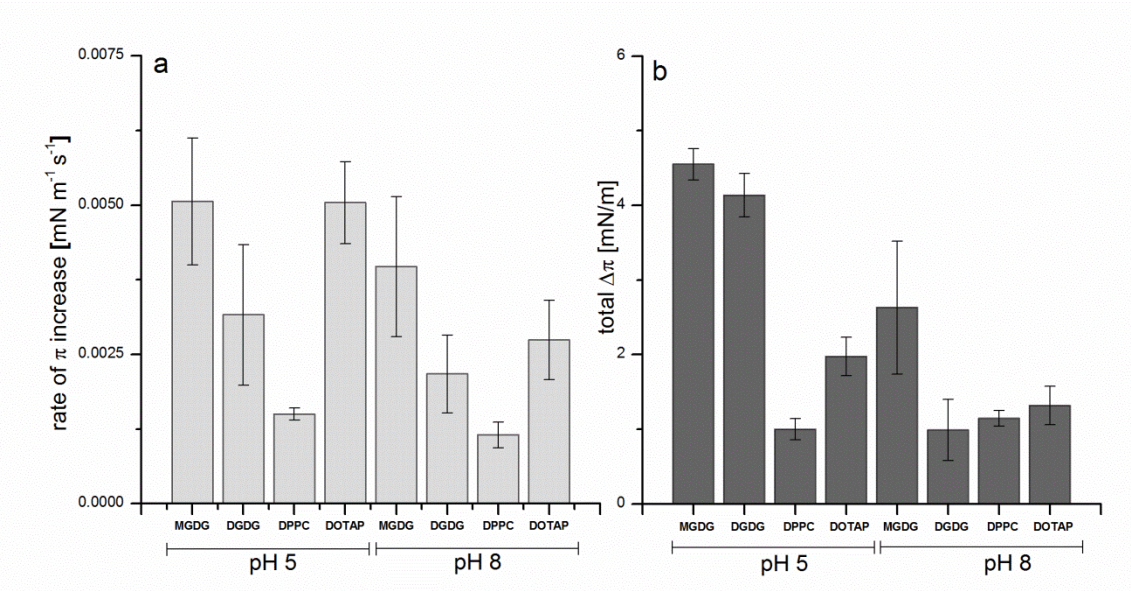

Fig. 2. The lFNR injection beneath the lipid monolayer: a comparison of rate of initial π increase (a) and the total change in π (b) for selected composition of the monolayer (MGDG, DGDG, DPPC or DOTAP) and two pH values (pH 5 and pH 8). Error bars – SD from 3-4 independent repetitions.

Pressure-area isotherms indicated that protein binding influenced the lipid behavior. We checked this effect for sFNR and MGDG or DGDG at both pH 5 and pH 8 (compare Supplementary Fig. S-4). For DGDG, a slight increase in the collapse area per molecule at pH 8 was observed. The stabilization of the membrane at pH 5 resulted in a collapse plateau. A similar behavior was found for MGDG monolayers. Almost no changes in the shape of curves were noted, indicating that the protein did not influence lipid reorganization during compression.

Temperature as a factor modulating binding of FNR to membranes.

Temperature is an important environmental factor, which modulates the function of photosynthetic membranes. It changes lipid fluidity as well as the reaction rates catalyzed by proteins. Here we checked how temperature influences sFNR binding to MGDG or DGDG monolayers, at pH 5 or at pH 8 (see Fig. S-

5). In all tested temperatures, the binding was faster at pH 5 for both lipids. The binding to MGDG was slower at pH 8 than at pH 5, except for 32°C. The maximum binding rate was found for MGDG at pH 5, at 28°C. At higher temperatures the binding rate decreased. For DGDG monolayers, the binding rate was almost zero at 10°C. It increased (faster at pH 5) to reach a plateau in the range of 30°C. The Arhenius plot (ln[binding rate] vs 1/T, not shown) was not linear, which indicates that at least two processes influenced the observed changes. One of them was most probably an increase in the protein diffusion rate, while the other was a change in the monolayer (e.g. resulting from faster lateral diffusion). In highest temperatures, changes in sFNR tertiary structure may also influence the observed rates.

Modulation of FNR binding by ferredoxin

One of the most important factors which should be considered in FNR membrane attachment-detachment is the presence of Fd. We tested FNR binding to membranes in the presence of model ferredoxins. Two *Arabidospis* Fd isoforms, namely Fd2 and Fd4, were chosen. Fd2 is homologous to photosynthetic ferredoxin, involved in linear electron transfer. Fd4 has a higher redox potential and is a rare case of ferredoxin, which is involved in different processes, including signaling and redox tuning. The results are presented in Fig. 3.

Fd2 did not influence sFNR binding to the membrane at pH 8 and slightly reduced FNR binding at pH 5. Fd2 alone slightly influenced membrane stability, but to a lower extent than FNR. Fd4 caused a more significant increase in π, especially at pH 8 and a reduction of FNR binding both at pH 5 and pH 8. This effect was especially substantial at pH 8.

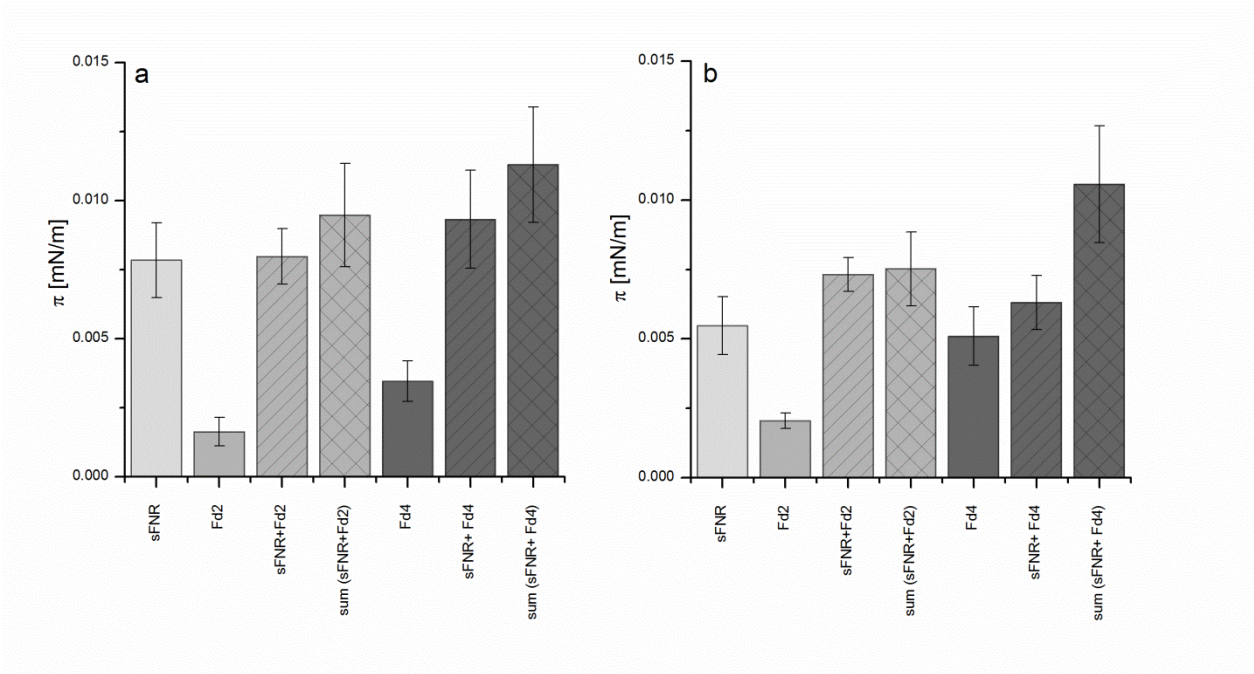

Fig. 3. Modulation of sFNR binding to the MGDG monolayer at pH 5 (a) or at pH 8 (b), by the presence of Fd2 or Fd4. Initial π was 10 mN/m. The legend to the bars: sFNR – the control injection of sFNR, Fd2/Fd4 – separate injections of respective ferredoxins. sFNR+Fd2/sFNR+Fd4 – the injection of a mixture (1:1 molar ratio) of sFNR and Fd2/Fd4. Bars labeled "Sum" represent a mathematic sum of values from separate injections

of sFNR and Fd2/Fd4. Error bars – SD from 3-4 independent repetitions, the sum error calculated from errors of separate injections by full derivative method.

Both Fd2 and Fd4 are reaction partners (electron donors or acceptors) for sFNR. This is observed as a significant increase in the rate of cytochrome c reduction by FNR (Fig. 4). The higher reaction rate in the presence of Fd2 is most probably related to the lower midpoint potential of this Fd, which makes it a more efficient electron donor. In the presence of liposomes, built up with pure DGDG or MGDG/DGDG, the electron transfer rate was reduced by about 20% in all tested variants. This suggests that the reduction resulted from the inhibition of NADPH binding by FNR (or electron transfer between FNR and the FAD cofactor of FNR) and not from the FNR-Fd interaction.

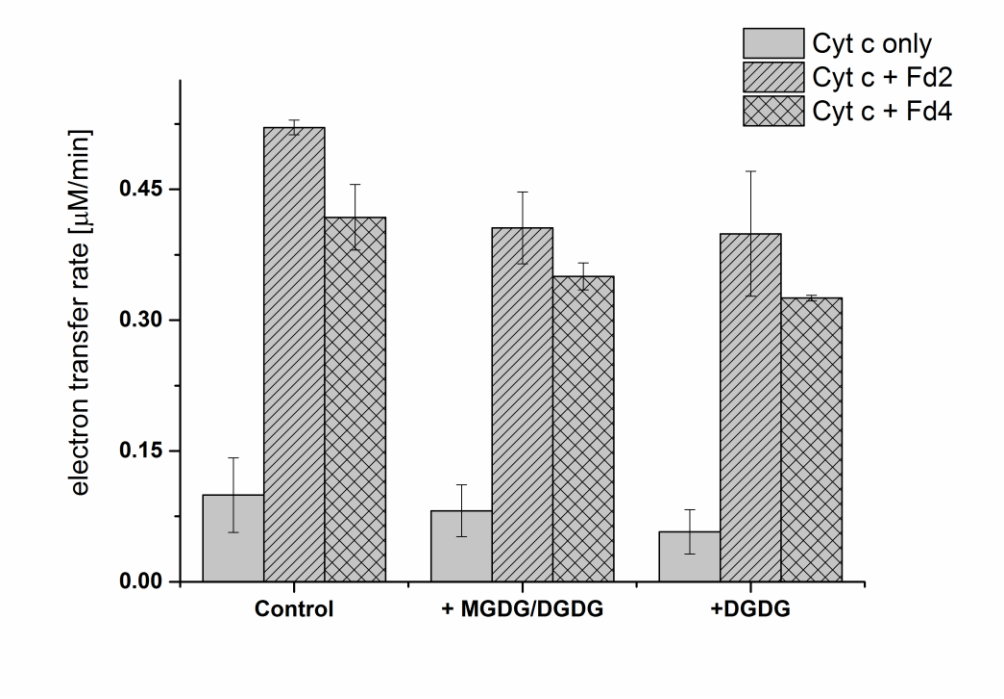

Fig. 4. The influence of lipids on the electron transfer rate between FNR and Fd2 or Fd4. The rate was determined by Fd-dependent cytochrome c reduction. Lipids were used in the form of multilamellar vesicles of pure DGDG or a mixture of MGDG/DGDG (30% MGDG/70% DGDG).

Modulation of FNR binding by NADPH and $NADP^+$

NADP is a natural substrate of FNR. The ratio between $NADP^+$ and NADPH is an important switch between cyclic and linear electron transfer. NADPH binding induces small conformational changes in FNR molecules. This is why we also tested the effect of NADP, both in its oxidized and reduced form, on FNR binding to membranes. We considered two situations – the nucleotide was added after the FNR injection or before it. Fig. 5 presents the results obtained from this experiment for injections beneath MGDG and DOTAP monolayers. Results for DGDG monolayers, as well as lFNR injection under the same set of lipids are shown in supplementary figures S-6 and S-7. Generally, the presence of NADPH decreased the biding rate and $\Delta\pi$, with the exception of lFNR at pH 8 injected beneath the DOTAP monolayer. $NADP^+$ caused no effect on the MGDG-binding rate at both pH, while it reduced sFNR binding to DGDG. This effect was stronger at pH 8. There was no significant influence of $NADP^+$ on lFNR binding at pH 5 but a reduction of the binding rate was observed at pH 8.

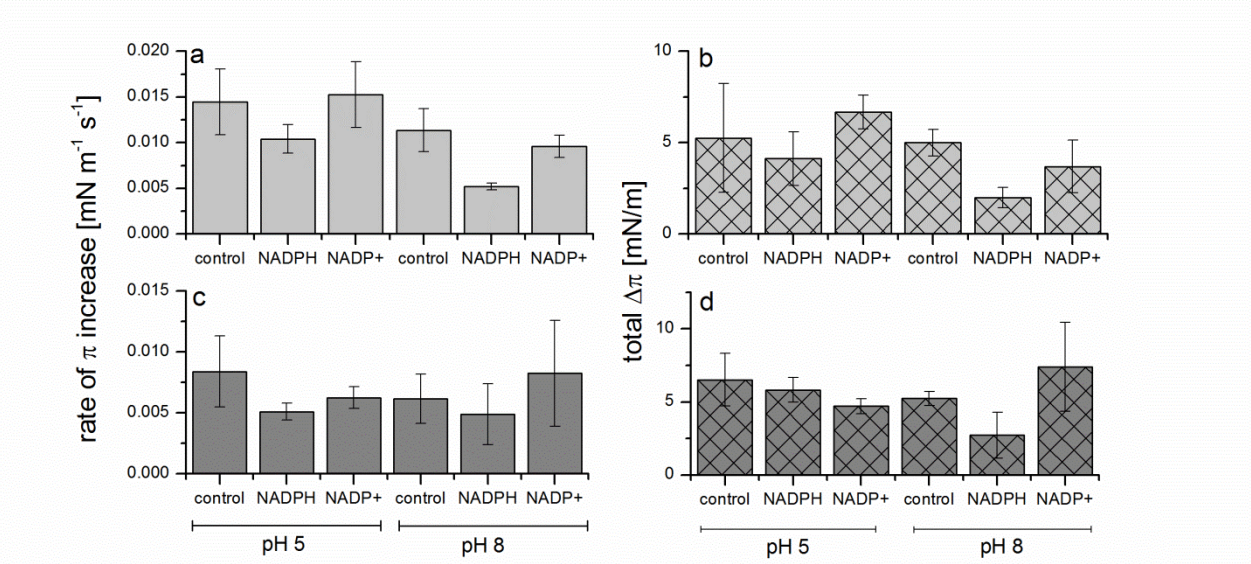

Fig.5. Modulation of sFNR binding: the rate of π increase (a, c) and total π change (b, d) to MGDG (a, b) or DOTAP (c ,d) by NADPH or $NADP^+$, at pH 5 or pH 8. $NADP^+$/NADPH (0.1 μM) was present before FNR injection.

Phycobilisomes influence on membrane binding

Phycobilisomes are huge protein complexes, in *Synechocystis sp.* composed mainly of phycocyanine. *In vitro* these complexes are stable at high phosphate concentration (0.75 M). This phosphate concentration is far from physiological, however it simulates the natural environment by preventing phycobilisome decomposition. Because the CpcD-like domain of lFNR is believed to interact with phycobilisomes [2], we tested how the presence of phycoblisomes (10 times molar concentration of FNR) influenced the binding. Fig. 6 presents example curves. Phycobilisomes did not significantly change the rate of binding of lFNR to the membrane, however high phosphate concentration significantly increased the binding rate. The presence of phycobilisomes reduced Δπ. This was not due to the change in the ionic strength, as high NaCl concentration (control to high phosphate) decreased the binding rate (see Supplementary, Fig. S-8).

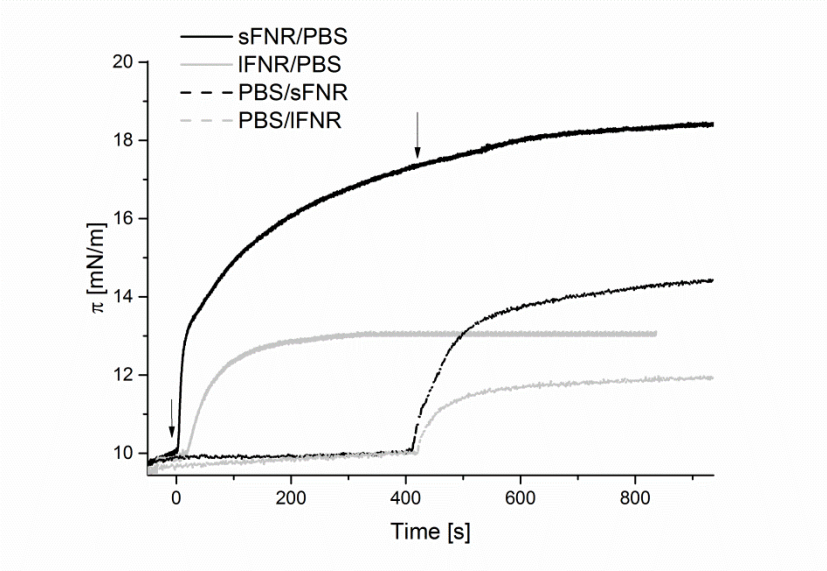

Fig.6. The influence of phycobiliosomes (PBS) on sFNR (black line) or lFNR (grey line) interaction with the DGDG monolayer, formed at π= 10 mN/m. The water phase was buffered with 0.75 M phosphate buffer, pH 8. Phycobilisomes were injected before (dashed lines) or after the FNR injection (solid lines). Arrows indicate FNR and PBS injections in the order depicted in the figure legend.

We also checked the pressure-area isotherms for DGDG formed at the surface of the 0.75 M phosphate buffered water phase. We examined each monolayer after the insertion of sFNR or PBS (Fig. S-9). No influence on the collapse pressure was observed except a slight decrease in the collapse area per molecule. An additional transition occurred at about 120 A^2/molecule. This may be interpreted as the reorganization of lipids with bound protein molecules.

Modulation of FNR binding by heavy metals

Heavy metals are also one of possible factors, which may shift photosynthetic electron transport form the linear to cyclic pathway, mainly because of photosystem II toxicity. Heavy metals are known to impact FNR activity. The presence of heavy metal ions (Cd^{2+}, Zn^{2+}, Cu^{2+}) did not change significantly FNR binding to the membrane, even at 1 mM concentration. At pH 8 this concentration of Cd^{2+}/Zn^{2+} caused respectively a moderate FNR inhibition [41]. Cu^{2+} inhibited FNR activity at low pH, while there was no Zn^{2+}-related inhibition and a much weaker inhibitory effect of Cd^{2+} [42]. Here we tested the influence of heavy metal ions on binding of FNR to membranes. We found that the injection of heavy metal salt solutions under the monolayer with already bound FNR did not change π. Cu^{2+} injection (1 mM) decreased π by 2-3 mN/m, both in control conditions and in the presence of the protein (see an example in Supplementary, Fig. S-10). For SQDG such a decrease was observed for all ions, including the control with NaCl and thus it may be related to the rearrangement of membranes after charge shielding. When FNR was preincubated with heavy metal ions (30 min, 1 mM concentration), we observed a decrease in the rate of binding.

Analysis of secondary structures of sFNR and lFNR in the presence of heavy metals

sFNR and lFNR interacted differently with membranes. We compared the Amid I band in the FTIR spectrum of these proteins (Fig. 7), which reflects the changes in their structures, after treatment with

heavy metal ions (Tab. I). Helices consist of 42% of sFNR and 39% of lFNR. After the heavy metal treatment, slight changes in secondary structures of both sFNR and lFNR were observed. Secondary structures were influenced differently depending on the ion type and the protein. Cadmium treatment of sFNR reduced mainly the amount of loops. Interestingly, incubation with ions did not induce aggregation, which would reflect protein denaturation. Denaturation, if present could lead to artifacts during membrane-interaction measurements. Small changes in protein structures were also found when tryptophan fluorescence of sFNR and lFNR molecules was investigated in the presence of heavy metals. There are five tryptophan residues within the sFNR molecule and none in the additional domain of lFNR. The residues are partially buried, thus the emission maximum is near 340 nm. Both cadmium and zinc present in the solution caused a decrease in the fluorescence intensity by about 10%. Almost no shift in the position of the emission maximum was observed. In the case of copper, due to its known quenching properties, the decrease of fluorescence intensity was about 80-90%. The example results obtained for sFNR are shown in supplementary (Fig. S-11).

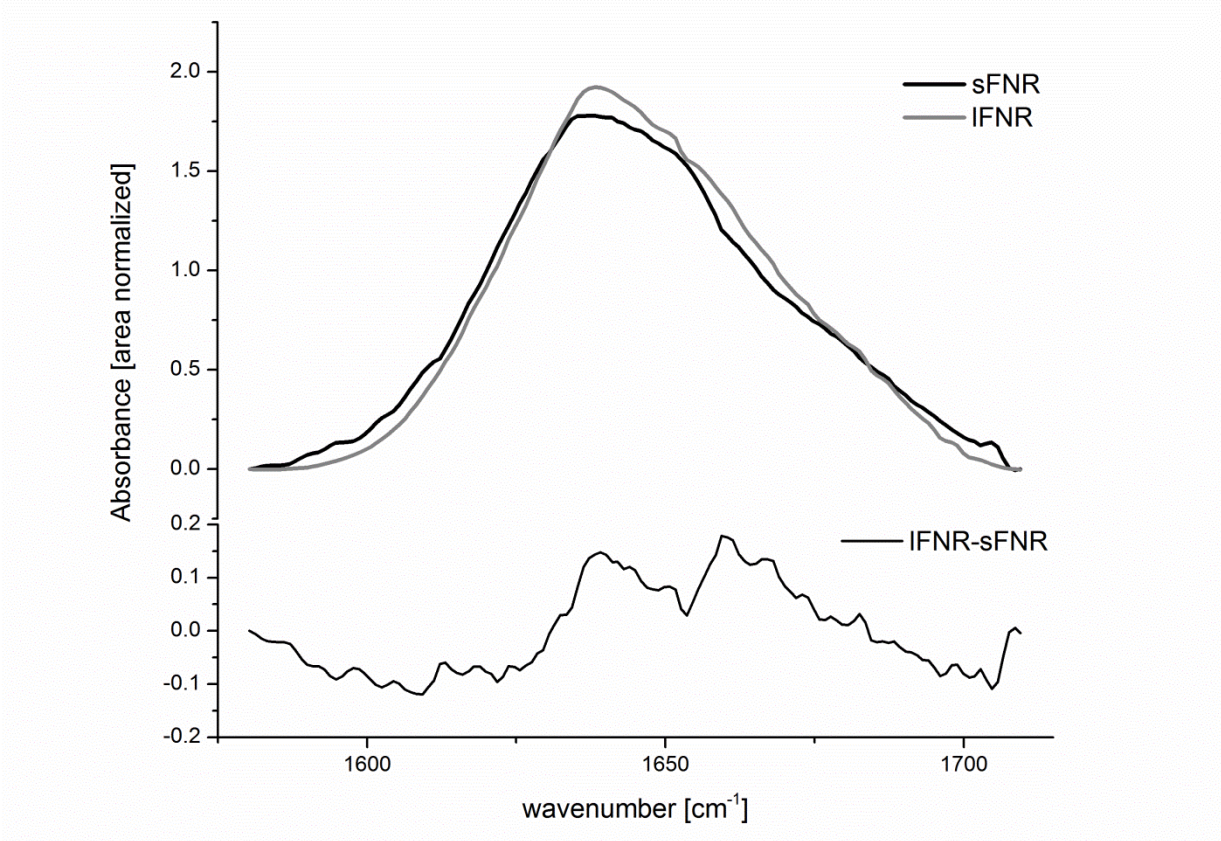

Fig.7. Amide I bands of sFNR and lFNR, area normalized. Below – the difference spectrum.

Table I. Secondary structure composition of sFNR and lFNR, treated with heavy metal ions, as predicted from Amide I bands deconvolution. Values represent the percentage of area of the Amid I band corresponding to given structural component.

	A-helix [%]		antiparallel β-sheets [%]		parallel β-sheets [%]		Loops [%]		Aggregates [%]	
	sFNR	lFNR	sFNR	lFNR	sFNR	lFNR	sFNR	lFNR	sFNR	lFNR
Control	41.48	39.55	3.47	4.56	6.30	6.73	3.49	3.63	2.70	2.78
+ Cd^{2+}	40.90	41.94	2.88	3.30	7.92	5.68	2.98	1.19	2.04	1.67
+ Zn^{2+}	39.56	39.03	4.22	4.49	7.24	7.39	2.99	2.91	2.38	2.48
+ Cu^{2+}	39.23	39.95	3.55	2.57	5.21	6.41	3.18	2.97	2.84	2.63

Analysis of FNR interaction with lipids in vesicles

Apart from binding to lipid monolayers, we also tested binding of FNR to lipids in vesicles. We performed sFNR precipitation with multilamellar vesicles (MLV), composed of DGDG or a MGDG-DGDG mixture (30% MGDG, 70% DGDG). The binding could be monitored by SDS-PAGE, which enabled to estimate the dissociation constant (K_d). The Kd was found to be below 0.1 µM at pH 5 and about 1.8 µM at pH 8. However, a high amount (up to 1000) of lipid molecules for one FNR molecule was estimated from these calculations. It seems very unlikely and most probably results from the method limitation. Firstly, FNR concentration is a limiting factor, due to SDS-PAGE detection sensitivity. Secondly, the pellet might be contaminated with the remaining solution. For more details, see Suplementary (Fig. S-12 and the related paragraph). We have verified this to some extent by isothermal titration calorimetry (ITC), finding the reaction exothermic, with Kd at nanomolar range for sFNR binding to MGDG-DGDG liposomes at pH 8. In this experiment, the sFNR molecule was found to bind to 25-30 lipid molecules. With assumption that most of liposomes used in the experiment is single bilayer, it may be postulated that one FNR molecule is bound to 12-15 lipid molecules. The data are shown in Supplementary (Fig. S-13 and S-14 and discussion there).

The interaction between sFNR/lFNR and small unilammelar vesicles (SUV) was investigated by gel filtration. This technique separates molecules dependent on their hydrodynamic radius. If a complex between SUV and FNR is formed, FNR specific absorption in the SUV fraction and a shift in the fraction position is observed. However, for all tested variants there were no significant changes in the elution profiles and no absorption at 459 nm was observed in liposome fractions (Fig. S-15). Surface binding could be disturbed by the high curvature of SUV as well as shearing between the gel beads.

The digestion by trypsin or proteinase K may be used to identify protein fragments, which are screened by lipids. In the presence of proteinase K, both in the control and in the presence of liposomes, FNR was digested into small peptides. In milder conditions, only a fragment of about 10 kDa was digested, but no difference was observed between the control and liposomes (Fig. S-16). Gel filtration of FNR digested in the presence or absence of liposomes (data not shown) confirmed that lipids did not interfere with the digestion.

FNR-membrane interaction measured by DPH anisotropy

DPH is a fluorophore, which localizes into the hydrophobic membrane region. Anisotropy of DPH is sensitive to membrane fluidity, which is influenced by the incorporation of proteins. Fig. 8 compares DPH anisotropy for liposomes incubated with FNR and the control ones. DPH anisotropy resembled the difference in fluidity between saturated DPPC and non-saturated DGDG, but not in the presence of FNR. The addition of MGDG did not facilitate to detect the FNR influence.

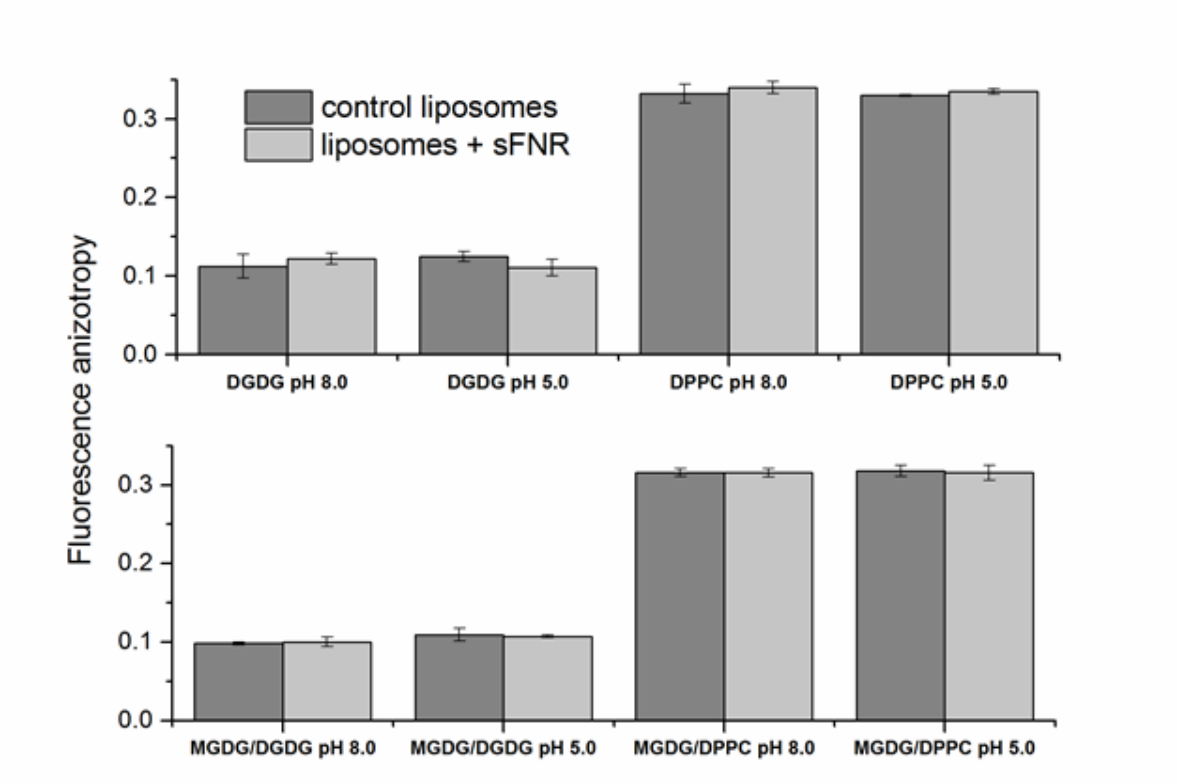

Fig. 8.The influence of sFNR on DPH anisotropy. Lipids – 100 μg/ml, DPH – 0.5 μg/ml, FNR – 0.4 μM. MGDG (in MGDG/DGDG and MGDG/DPPC mixtures) was added to 30% of molar concentration. Buffer conditions as in previous experiments.

Discussion

Here we provided a detailed analysis of *in vitro* interaction between *Synechocystis* PCC 6803 FNR (both sFNR and lFNR) and model lipid membranes, namely lipid monolayers and liposomes, in the presence of factors which may potentially modulate this process: the pH change, the temperature change, the presence of ferredoxin, $NADP^+$ and NADPH as well as cadmium, copper and zinc ions. Heavy metal ions were chosen to simulate stress conditions. For the long FNR form, we also included phycobilisomes as a modulating factor. We used sFNR as an FNR model due to its structure homology with other photosynthetic FNRs. For binding to monolayers, we determined the binding rate and the total change of π, which may be interpreted as a semi-quantitative estimation of the amount of bound protein molecules. We proved binding to all tested lipids. However, the binding rate depends on the lipid type, the packing of membrane represented by the initial surface pressure value and pH of the water phase. The fastest binding was observed for less packed MGDG (initial π = 10 mN/m) at pH 5. Second and third binding rates were determined for DPPC and DOTAP monolayers respectively. lFNR binding to DOTAP was as fast as to MGDG and the binding to DGDG was faster than to DPPC. Interestingly, the total change of π was not significantly different, which suggests that time is the only limiting factor in this process. At pH 8 the binding was less effective than at pH 5. Both the rate and Δπ were reduced, but this difference was more pronounced for sFNR.

The difference between the binding to MGDG and DGDG was previously shown for spinach FNR [22]. The modulation of *Synechocystis* FNR binding by pH is similar to the one described for spinach FNR. The interaction with these lipids may be assumed to be natural, as both MGDG and DGDG are present in thylakoids. However, here we found that FNR binds also to DPPC and other PC lipids, which are absent in the protein's natural environment. Moreover, the binding to DPPC is even faster than the binding to DGDG. Both DGDG and DPPC are bilayer forming lipids, while MGDG forms inverted hexagonal structures (H_{II}). H_{II} structures are very important for biological membranes [27], facilitating protein fitting into the bilayer. The stronger interaction of FNR with MGDG suggests that this binding is dependent on the type of membrane organization, rather than the type of the head group. This may be explained by protein stacking between head groups. The protein uses the free space which is left between head groups of lipids in the hexagonal phase. The hypothesis is supported by generally lower binding rates for more packed monolayers (π=20 mN/m *vs* 10 mN/m). Also, the multicomponent changes in the binding rate in the function of temperature suggest, that membrane fluidity may be one of the factors important for protein binding.

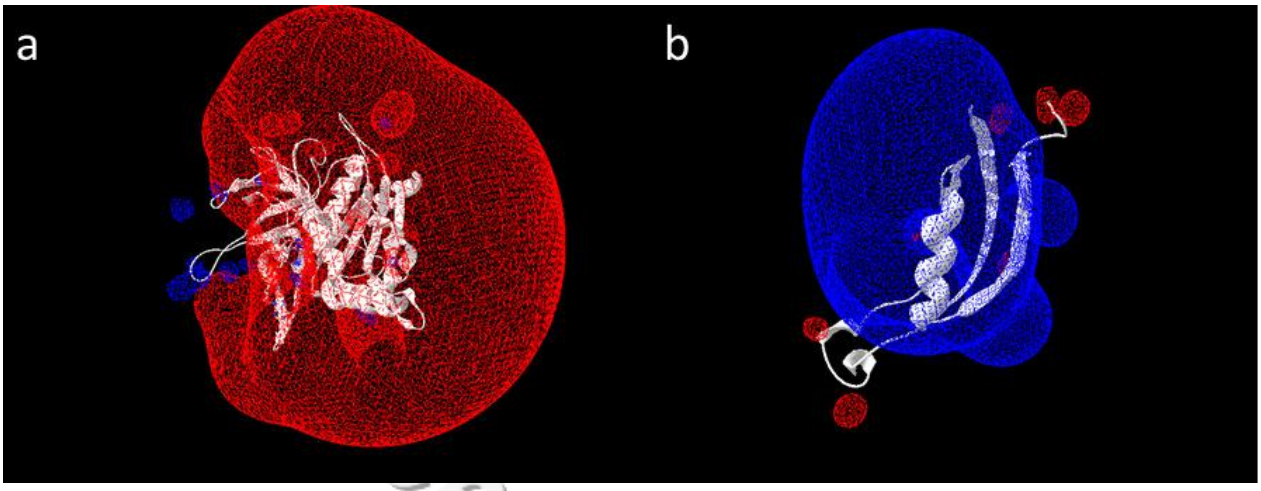

Fig. 9. Equipotential surfaces (red – negative (-1.8 V), blue – positive (+1.8 V) calculated for sFNR (a) and the cpcD-like domain of lFNR (b). The potential was calculated for the default protonation of the protein at pH 7, the dielectric constant of solvent 80, the dielectric constant of protein 4 and the solvent ionic strength 50 mM.

We also showed that charged lipids do attract FNR. It is quite common in nature, that the interaction between negative and positive patches on molecules defines the orientation of complexes and bigger structures. We observed FNR biding to both positively charged (DOTAP) and negatively charged lipids (SQDG and PG). This result is perplexing in terms of theories depicting the orientation of proteins and their binding partners. FNR behavior may be the result of the presence of differently charged patches on the protein molecule. Known FNR molecules are mostly negatively charged, with small positive patches – namely in the Fd docking site. *Synechocystis* FNR has not been crystalized yet, but we were able to obtain its model based on the homology with *Synechococcus* FNR (pdb: 2b5o). The surface electrostatic potential (Fig. 9) calculated for this model clearly shows that *Synechocystis* FNR molecules have most of their surface negatively charged with a small amount of positive charge in the putative Fd binding site. This may explain the interaction with both negatively and positively charged lipids. However, the comparison of the ratio of negative to positive patches suggests that binding to positively charged DOTAP should be much stronger than to PG or SQDG, which is not the case.

Additionally, we observed that high NaCl concentration significantly reduced FNR binding to monolayers. The conditions were non-native, but they provided some information about the nature of the FNR-membrane interaction. This experiment suggests that several charged amino acids are involved in the binding driving force. Charged residues may be screened by Na^+/Cl^- ions, as was described for the FNR-Fd binding site [43], [44]. The general charge of a protein molecule also modulates the binding, which is reflected by the comparison of sFNR and lFNR binding rates. lFNR has a higher isoelectric point (theoretical pI 5.72 versus 5.27 for sFNR) and a lower overall molecular charge (see Fig. 9b presenting the equipotential surfaces on the cpcD-like domain). This is most probably the reason for its lower rate of binding to the membrane. The presence of Na^+/Cl^- ions may strengthen the hydrophobic interaction by weakening the electrostatic driving force. Since in the presence of elevated NaCl we did not observe any increase in the binding rate, we may hypothesize that hydrophobic interactions are not the main driving force, at least in the initial phase of membrane attachement. In ITC experiment, we observed exotermic binding between sFNR/lFNR and DGDG/MGDG liposomes, acoompanied by negative ΔH. Such

charcetristics is also an evidence of significant electrostatic contribution into binding, as it was shown e.g. for beta-amyloid and phospholipids interactions {Terzi, 1994 #1212} or for milk protein interacting with polysaccharides {Turgeon, 2007 #1213}.

Not only have we shown that electrostatics is the driving force behind binding, but also that binding is restricted to the lipid head groups. The measurement of DPH anisotropy did not show any significant changes in the presence of FNR. Even prolonged incubation time did not influence this parameter. The MGDG and DGDG isotherms of compression were not altered significantly in the presence of FNR. This also suggests that the protein is not incorporated into the monolayer. In a previous study, devoted to the analysis of spinach FNR binding to MGDG and DGDG bilayers we proved that lipid head groups should be taken into account as an incorporation place, since FNR activity was only slightly impaired in the presence of liposomes [22]. This binding is rather unstable, as we did not find FNR bound to liposomes during the analysis by gel filtration (see also K_d discussion in Supplementary). It may be explained either by a strong disturbance in the equilibrium caused by dilution during on-column separation or by distraction of FNR-liposome complexes by beads (e.g. by combined friction and electrostatic attraction). The monolayer technique we applied here allows to perform measurements at a much lower lipid density than the one in liposomes. We carried out measurements at 10 mN/m and 20 mN/m, which is much lower than the collapse conditions [45]. However, in most cases we detected at least twice as fast binding at lower π. More free space between lipid head groups is the most probable explanation of the differences between binding to monolayers and liposomes.

Assuming that FNR direct binding to the lipid part of the membrane is responsible for changing the electron route in chloroplasts, it should be sensitive to factors that switch between the linear and cyclic electron transfer. These factors include the presence of ferredoxin and excess of NADPH. We showed that both Fd2 and Fd4 were efficient reaction partners for ferredoxin. The presence of lipids decreased, by a similar factor the rate of electron transfer between FNR and Fd2 or Fd4. However, we found that only Fd4, which has a higher midpoint potential than typical photosynthetic ferredoxin (Fd2), decreased the FNR- membrane binding rate. This Fd was also binding to the membrane and the total effect of the FNR binding rate reduction is rather related to the destabilization of the membrane by Fd than to the direct disturbance of FNR binding. The fact that ferredoxins alone bind to the membrane is interesting. The observed much higher binding of Fd4 suggests that the strength of membrane interaction may be one of the differences between Fd isoforms important for their functions .

We also found that NADPH reduces the sFNR and lFNR binding rate to MGDG and DGDG and in most cases to DOTAP. $NADP^+$ has an reducing effect only on binding to DGDG . In nature, the presence of $NADP^+$ should promote linear electron transfer and FNR binding to its binding place in the photosystem I [46]. Thus the observed changes in sFNR and lFNR behavior may be related to conformational changes occurring in the enzyme molecules after NADP binding [47, 48]. Interestingly, these changes are mostly restrained to remodeling of the enzyme active center, but this may also influence the electrostatic potential of the whole molecule. This was already discussed as an important constituent of the binding driving force. The stronger effect of NADPH may result from an additional reduction (charge transfer) of the FAD coenzyme of FNR. High phosphate (but not high NaCl) concentration promoted binding. Phosphate ions may partially bind to the NADP binding site. Since phosphate showed an effect opposite

to this of NADP, the phenomenon most probably results from membrane destabilization which facilitates binding, rather than from the influence of the enzyme.

Heavy metal ions are also considered to affect the transition between linear and cyclic electron transfer. They may change the secondary and tertiary structure of FNR [49]. Indeed, we showed that cadmium, copper and zinc influence the secondary structure composition of both sFNR and lFNR. Heavy metal ions slightly influenced α-helices, but had a stronger impact on more flexible elements – loops and β-sheets. The decrease in the content of loops may explain the reduced binding rate observed for FNR preincubated with metal ions. Heavy metals are also known to induce protein aggregation [50]. The aggregation of FNR molecules may influence the binding rate by screening the patches on the protein surface involved in the interaction with the membrane. However, this is not the case here, since analysis of FT-IR spectra not show elevated levels of aggregates. Because FT-IR spectra may not always be sensitive to aggregation, we also confirmed this conclusion by measurement of tryptophane fluorescence.

To sum up, we tested sFNR and lFNR binding to several lipids, differing by head group properties and bilayer forming tendency. We found that FNR binds only to the head group region and a larger space available between head groups facilitates the binding. Electrostatic attraction is important for the driving force. However, the binding is not restricted to charged lipids. Both NADPH and $NADP^+$ decrease the binding rate, probably by inducing conformational changes in the enzyme molecule. Ferredoxin 4 with E_m of -150 mV, but not the typical photosynthetic Fd2, reduces the FNR-membrane binding rate. Those findings enable us to conclude, that for both sFNR and lFNR the specific direct binding to the lipid part of the membrane *in vivo* is not of primary importance. However, it should be still taken into account when performing *in vitro* studies using lipids and FNR, as binding may be induced and modulated *in vitro* by several factors.

Acknowledgements:

Presented work was financed by Iuventus PLUS grant no 0166/IP/2011/71 from Ministry of Science and Higher Education, Poland. Measurements were partially performed in the NanoFun laboratories co-financed by the European Regional Development Fund within the Innovation Economy Operational Programme POIG.02.02.00-00-025/09. This work was conducted while a Postdoctoral Fellow of KG at the Institute of Physics University of Marie Sklodowska-Curie, sponsored by the National Science Centre through FUGA 2013/08/S/NZ1/00823. JG acknowledges that most of the experimental part of presented work was done during her employment in Institute of Physics PAS. Authors are grateful to dr Ksenia Maximowa and prof. Joanna Trylska form CENT, UW, for access to apparatus and assistance with ITC measurements.

Literature:

[1] N. Carrillo, E.A. Ceccarelli, Open questions in ferredoxin-NADP+ reductase catalytic mechanism, Europ J Biochem, 270 (2003) 1900-1915.
[2] J.J. van Thor, R. Jeanjean, M. Havaux, K.A. Sjollema, F. Joset, K.J. Hellingwerf, H.C. Matthijs, Salt shock-inducible photosystem I cyclic electron transfer in Synechocystis PCC6803 relies on binding of ferredoxin: NADP+ reductase to the thylakoid membranes via its CpcD phycobilisome-linker homologous N-terminal domain, BBA-Bioenergetics, 1457 (2000) 129-144.
[3] W.M. Schluchter, D.A. Bryant, Molecular characterization of ferredoxin-NADP+ oxidoreductase in cyanobacteria: cloning and sequence of the petH gene of Synechococcus sp. PCC 7002 and studies on the gene product, Biochemistry, 31 (1992) 3092-3102.
[4] Y. Munekage, M. Hashimoto, C. Miyake, K.-I. Tomizawa, T. Endo, M. Tasaka, T. Shikanai, Cyclic electron flow around photosystem I is essential for photosynthesis, Nature, 429 (2004) 579-582.
[5] H. Zhang, J.P. Whitelegge, W.A. Cramer, Ferredoxin: NADP+ Oxidoreductase Is a Subunit of the Chloroplast Cytochrome b6fComplex, J Biol Chem, 276 (2001) 38159-38165.
[6] Y. Shahak, D. Crowther, G. Hind, The involvement of ferredoxin-NADP+ reductase in cyclic electron transport in chloroplasts, BBA-Bioenergetics, 636 (1981) 234-243.
[7] P. Joliot, A. Joliot, Cyclic electron transfer in plant leaf, Proc Nat Acad Sci USA, 99 (2002) 10209-10214.
[8] R.E. Cleland, D.S. Bendall, Photosystem I cyclic electron transport: measurement of ferredoxin-plastoquinone reductase activity, Photosynthesis Res, 34 (1992) 409-418.
[9] A.P. Hertle, T. Blunder, T. Wunder, P. Pesaresi, M. Pribil, U. Armbruster, D. Leister, PGRL1 is the elusive ferredoxin-plastoquinone reductase in photosynthetic cyclic electron flow, Mol Cell, 49 (2013) 511-523.
[10] Y. Munekage, M. Hojo, J. Meurer, T. Endo, M. Tasaka, T. Shikanai, PGR5 is involved in cyclic electron flow around photosystem I and is essential for photoprotection in Arabidopsis, Cell, 110 (2002) 361-371.
[11] M. Iwai, K. Takizawa, R. Tokutsu, A. Okamuro, Y. Takahashi, J. Minagawa, Isolation of the elusive supercomplex that drives cyclic electron flow in photosynthesis, Nature, 464 (2010) 1210-1213.
[12] L. Vojta, D. Carić, V. Cesar, J.A. Dunić, H. Lepeduš, M. Kveder, H. Fulgosi, TROL-FNR interaction reveals alternative pathways of electron partitioning in photosynthesis, Sci Reports, 5 (2015).

[13] S. Juric, K. Hazler-Pilepic, A. Tomasic, H. Lepedus, B. Jelicic, S. Puthiyaveetil, T. Bionda, L. Vojta, J.F. Allen, E. Schleiff, H. Fulgosi, Tethering of ferredoxin:NADP+ oxidoreductase to thylakoid membranes is mediated by novel chloroplast protein TROL, Plant J, 60 (2009) 783-794.
[14] J.P. Benz, M. Lintala, J. Soll, P. Mulo, B. Bolter, A new concept for ferredoxin-NADP(H) oxidoreductase binding to plant thylakoids, Trends Plant Sci, 15 (2010) 608-613.
[15] J. Benz, A. Stengel, M. Lintala, Y.-H. Lee, A. Weber, K. Philippar, I. Gügel, S. Kaieda, T. Ikegami, P. Mulo, Arabidopsis Tic62 and ferredoxin-NADP (H) oxidoreductase form light-regulated complexes that are integrated into the chloroplast redox poise, Plant Cell, 21 (2009) 3965-3983.
[16] G.T. Hanke, Y. Kimata-Ariga, I. Taniguchi, T. Hase, A post genomic characterization of Arabidopsis ferredoxins, Plant Physiol, 134 (2004) 255-264.
[17] S. Jokipii-Lukkari, A.J. Kastaniotis, V. Parkash, R. Sundström, N. Leiva-Eriksson, Y. Nymalm, O. Blokhina, E. Kukkola, K.V. Fagerstedt, T.A. Salminen, Dual targeted poplar ferredoxin NADP+ oxidoreductase interacts with hemoglobin 1, Plant Sci, 247 (2016) 138-149.
[18] M. Bojko, J. Kruk, S. Więckowski, Plastoquinones are effectively reduced by ferredoxin:NADP+ oxidoreductase in the presence of sodium cholate micelles Significance for cyclic electron transport and chlororespiration, Phytochemistry, 64 (2003) 1055-1060.
[19] M. Bojko, S. Wieckowski, Three substrate binding sites on spinach ferredoxin : NADP(+) oxidoreductase. Studies with selectively acting inhibitors, Photosynthetica, 39 (2001) 553-556.
[20] M. Bojko, S. Wieckowski, NADPH and ferredoxin : NADP(+) oxidoreductase-dependent reduction of quinones and their reoxidation, Phytochemistry, 50 (1999) 203-208.
[21] R. Szymańska, J. Dłużewska, I. Ślesak, J. Kruk, Ferredoxin: NADP+ oxidoreductase bound to cytochrome b6f complex is active in plastoquinone reduction: Implications for cyclic electron transport, Physiologia plantarum, 141 (2011) 289-298.
[22] J. Grzyb, M. Gagos, W.I. Gruszecki, M. Bojko, K. Strzalka, Interaction of ferredoxin:NADP+ oxidoreductase with model membranes, BBA, 1778 (2008) 133-142.
[23] J.W. Heemskerk, H. Schmidt, U. Hammer, E. Heinz, Biosynthesis and desaturation of prokaryotic galactolipids in leaves and isolated chloroplasts from spinach, Plant physiology, 96 (1991) 144-152.
[24] P. van der Sluijs, M. Hull, P. Webster, P. Mâle, B. Goud, I. Mellman, The small GTP-binding protein rab4 controls an early sorting event on the endocytic pathway, Cell, 70 (1992) 729-740.
[25] J.E. Johnson, R.B. Cornell, Amphitropic proteins: regulation by reversible membrane interactions (review), Mol Membrane Biol, 16 (1999) 217-235.
[26] P. Dörmann, C. Benning, Galactolipids rule in seed plants, Trends in plant science, 7 (2002) 112-118.
[27] J. Jouhet, Importance of the hexagonal lipid phase in biological membrane organization, Frontiers Plant Sci, 4 (2013) 494.
[28] R. Goss, M. Lohr, D. Latowski, J. Grzyb, A. Vieler, C. Wilhelm, K. Strzalka, Role of hexagonal structure-forming lipids in diadinoxanthin and violaxanthin solubilization and de-epoxidation, Biochemistry, 44 (2005) 4028-4036.
[29] M. Gabruk, B. Myśliwa-Kurdziel, J. Kruk, MGDG, PG and SQDG regulate the activity of light-dependent protochlorophyllide oxidoreductase, Biochem J, (2017) BCJ20170047.
[30] D. Latowski, J. Kruk, K. Burda, M. Skrzynecka-Jaskier, A. Kostecka-Gugała, K. Strzałka, Kinetics of violaxanthin de-epoxidation by violaxanthin de-epoxidase, a xanthophyll cycle enzyme, is regulated by membrane fluidity in model lipid bilayers, Europ J Biochem, 269 (2002) 4656-4665.
[31] R. Worch, J. Krupa, A. Filipek, A. Szymaniec, P. Setny, Three conserved C-terminal residues of influenza fusion peptide alter its behavior at the membrane interface, BBA-General Subjects, 1861 (2017) 97-105.
[32] Z. Leonenko, E. Finot, H. Ma, T. Dahms, D. Cramb, Investigation of temperature-induced phase transitions in DOPC and DPPC phospholipid bilayers using temperature-controlled scanning force microscopy, Biophys J, 86 (2004) 3783-3793.

[33] K. Mitra, I. Ubarretxena-Belandia, T. Taguchi, G. Warren, D.M. Engelman, Modulation of the bilayer thickness of exocytic pathway membranes by membrane proteins rather than cholesterol, Proc Nat Acad Sci USA, 101 (2004) 4083-4088.
[34] J.P. Williams, G.R. Watson, S.P. Leung, Galactolipid Synthesis in Vicia faba Leaves II. Formation and Desaturation of Long Chain Fatty Acids in Phosphatidylcholine, Phosphatidylglycerol, and the Galactolipids, Plant Physiol, 57 (1976) 179-184.
[35] J.J. van Thor, T.H. Geerlings, H.C. Matthijs, K.J. Hellingwerf, Kinetic evidence for the PsaE-dependent transient ternary complex photosystem I/ferredoxin/ferredoxin: NADP+ reductase in a cyanobacterium, Biochemistry, 38 (1999) 12735-12746.
[36] E. Gantt, C.A. Lipschultz, J. Grabowski, B.K. Zimmerman, Phycobilisomes from blue-green and red algae isolation criteria and dissociation characteristics, Plant Physiol, 63 (1979) 615-620.
[37] M. Biasini, S. Bienert, A. Waterhouse, K. Arnold, G. Studer, T. Schmidt, F. Kiefer, T.G. Cassarino, M. Bertoni, L. Bordoli, SWISS-MODEL: modelling protein tertiary and quaternary structure using evolutionary information, Nucl Acid Res, (2014) gku340.
[38] L. Bordoli, F. Kiefer, K. Arnold, P. Benkert, J. Battey, T. Schwede, Protein structure homology modeling using SWISS-MODEL workspace, Nature Protocols, 4 (2009) 1-13.
[39] W. Reuter, G. Wiegand, R. Huber, M.E. Than, Structural analysis at 2.2 Å of orthorhombic crystals presents the asymmetry of the allophycocyanin–linker complex, AP· LC7. 8, from phycobilisomes of Mastigocladus laminosus, Proc Nat Acad Sci USA, 96 (1999) 1363-1368.
[40] N. Guex, M.C. Peitsch, T. Schwede, Automated comparative protein structure modeling with SWISS-MODEL and Swiss-PdbViewer: A historical perspective, Electrophoresis, 30 (2009) S162-S173.
[41] J. Grzyb, M. Bojko, A. Waloszek, K. Strzalka, Ferredoxin: NADP+ oxidoreductase as a target of Cd2+ inhibitory action - Biochemical studies, Phytochemistry, 72 (2011) 14-20.
[42] J. Grzyb, A. Waloszek, D. Latowski, W. S, Effect of cadmium on ferredoxin : NADP(+) oxidoreductase activity, J Inorg Biochem, 98 (2004) 1338-1346.
[43] A.R. De Pascalis, I. Jelesarov, F. Ackermann, W.H. Koppenol, M. Hirasawa, D.B. Knaff, H.R. Bosshard, Binding of ferredoxin to ferredoxin:NADP+ oxidoreductase: the role of carboxyl groups, electrostatic surface potential, and molecular dipole moment, Protein Sci, 2 (1993) 1126-1135.
[44] M. Kinoshita, J.Y. Kim, S. Kume, Y. Lin, K.H. Mok, Y. Kataoka, K. Ishimori, N. Markova, G. Kurisu, T. Hase, Energetic basis on interactions between ferredoxin and ferredoxin NADP+ reductase at varying physiological conditions, Biochim Biophys Res Comm, (2016).
[45] J. Zhang, C. Lo, P. Somasundaran, J.W. Lee, Encyclopedia of Surface and Colloid Science, (2002).
[46] B. Andersen, H.V. Scheller, B.L. Møller, The PSI-E subunit of photosystem I binds ferredoxin: NADP+ oxidoreductase, FEBS letters, 311 (1992) 169-173.
[47] Z. Deng, A. Aliverti, G. Zanetti, A.K. Arakaki, J. Ottado, E.G. Orellano, N.B. Calcaterra, E.A. Ceccarelli, N. Carrillo, P.A. Karplus, A productive NADP+ binding mode of ferredoxin–NADP+ reductase revealed by protein engineering and crystallographic studies, Nat Structural Mol Biol, 6 (1999) 847-853.
[48] C.M. Bruns, A.P. Karplus, Refined crystal structure of spinach ferredoxin reductase at 1.7 Å resolution: oxidized, reduced and 2′-phospho-5′-AMP bound states, J Mol Biol, 247 (1995) 125-145.
[49] J. Grzyb, M. Gagos, B. Mysliwa-Kurdziel, M. Bojko, W.I. Gruszecki, A. Waloszek, K. Strzalka, Cadmium inhibitory action leads to changes in structure of ferredoxin:NADP(+) oxidoreductase, J Biol Phys, 38 (2012) 415-428.
[50] N. Sakaib, M. Yaob, I. Tanakab, I. Kumagaia, Structural implications for heavy metal-induced reversible assembly and aggregation of a protein: the case of Pyrococcus horikoshii CutA1, FEBS letters, 556 (2004) 174.